Supporting information

# Facile non-fullerene acceptors for efficient photocatalytic hydrogen evolution

Xiaojian Zheng[a,+], Wenqin Si[b,+], Jiaqi Huang[a], Yuang Fu[c], Midhuna Sobhana Joy[d], Jiayu Wang[e], Tonghui Wang[f], Xun Xiao[a], Paul Hume[g], Kai Chen[d], Xinhui Lu[c], Yuze Lin[b,*], Xiaowei Zhan[a,*]

[a]State Key Laboratory of Advanced Waterproof Materials, School of Materials Science and Engineering, Peking University, Beijing 100871, China

[b]Beijing National Laboratory for Molecular Sciences, CAS Key Laboratory of Organic Solids, Institute of Chemistry, Chinese Academy of Sciences, Beijing 100190, China

[c]Department of Physics, The Chinese University of Hong Kong, New Territories, Hong Kong, China

[d]Robinson Research Institute, Victoria University of Wellington, Wellington 6012, New Zealand

[e]College of Polymer Science and Engineering, National Key Laboratory of Advanced Polymer Materials, Sichuan University, Chengdu 610065, China

[f]Key Laboratory of Automobile Materials, Ministry of Education, School of Materials Science and Engineering, Jilin University, Changchun 130022, China

[g]MacDiarmid Institute for Advanced Materials and Nanotechnology, School of Chemical and Physical Sciences, Victoria University of Wellington, Wellington, 6012, New Zealand

## Materials and synthesis

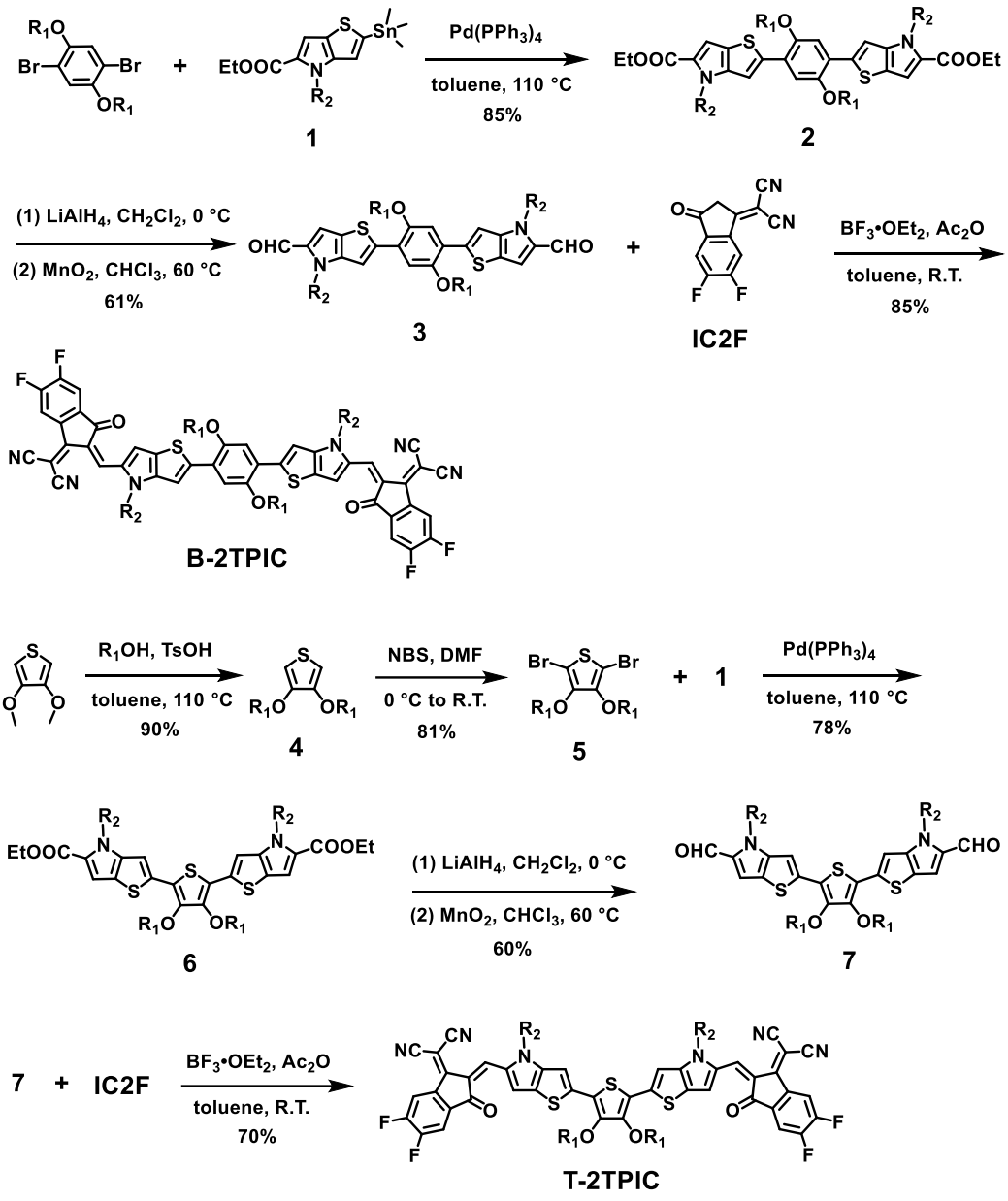


**Scheme S1.** Synthesis routes of B-2TPIC and T-2TPIC.

Unless stated otherwise, all the solvents and chemical reagents used were obtained commercially and were used without further purification. Toluene and tetrahydrofuran (THF) were distilled from sodium benzophenone under argon prior to use. 3,4-Dimethoxythiophene was purchased from Bide Pharmatech Ltd. 1,4-Dibromo-2,5-bis[(2-ethylhexyl)oxy]benzene was purchased from Shanghai Haohong Biological Pharmaceutical Technology Co., Ltd. Compound **1**[S1] and 3-(1,1-dicyanomethylene)-

5,6-difluoro-1-indanone (IC2F)[S2] were synthesized according to our previous works. PM6 was purchased from Solarmer Material Inc. PDINN was purchased from HyperPV Technology Co., Ltd.

*Synthesis of compound **2***

To a dry three-necked round flask was added compound **1** (0.33 M in toluene, 7.2 mL, 2.4 mmol), 1,4-dibromo-2,5-bis[(2-ethylhexyl)oxy]benzene (490 mg, 1.00 mmol) and dry toluene (10 mL). After deoxygenated with argon for 20 min, $Pd(PPh_3)_4$ (58 mg, 0.050 mmol) was added and then deoxygenated with argon for another 20 min. The reaction mixture was stirred at reflux for 24 h. After cooling, the mixture was extracted with $CH_2Cl_2$ (50 mL × 3) and the organic layer was dried over anhydrous $Na_2SO_4$ and filtered. After removing the solvent under reduced pressure, the residue was purified by column chromatography on silica gel using petroleum ether: $CH_2Cl_2$ (6:1, v/v) as the eluent yielding yellow oil (880 mg, 83%). $^1$H NMR (600 MHz, $CDCl_3$): $\delta$ 7.12 (s, 2H), 7.03 (s, 2H), 7.01 (s, 2H), 4.41 (d, $J$ = 7.6 Hz, 4H), 4.34 (q, $J$ = 7.1 Hz, 4H), 3.81 (m, 4H), 2.06–1.99 (m, 2H), 1.78–1.71 (m, 2H), 1.55–1.19 (m, 54H), 0.99–0.85 (m, 24H). MS (MALDI-TOF): $m/z$ 1057.69 $[MH]^+$.

*Synthesis of compound **3***

To a dry three-necked round bottom flask were added compound **2** (0.53 g, 0.50 mmol) and dry $CH_2Cl_2$ (10 mL). The mixture was deoxygenated with argon for 20 min. A solution of $LiAlH_4$ (1.0 M in THF, 1.42 mL, 1.42 mmol) was added dropwise at 0 °C. The mixture was stirred at 0 °C for 2 h. A saturated NaOH aqueous solution (10 mL) was added and the mixture was extracted with EtOAc (30 mL × 3). The organic layer was dried over anhydrous $Na_2SO_4$ and filtered. After removing the solvent, the residue was dissolved in $CHCl_3$ again, and $MnO_2$ (1.09 g, 1.25 mmol) was added in a dry three-necked round bottom flask under argon. The mixture was deoxygenated with argon for 20 min and was refluxed overnight. After cooling to room temperature, the reaction mixture was filtered through a pad of celite and the filtrate was dried over anhydrous

$Na_2SO_4$ and filtered. After removing the solvent, the residue was purified by column chromatography on silica gel using petroleum ether: $CH_2Cl_2$ (2:1, v/v) as eluent yielding yellow solid (296 mg, 61%). $^1$H NMR (600 MHz, $CDCl_3$): $\delta$ 9.97 (s, 2H), 7.12 (s, 2H), 7.03 (s, 2H), 7.01 (s, 2H), 4.41 (d, $J$ = 7.6 Hz, 4H), 3.81 (m, 4H), 2.06–1.99 (m, 2H), 1.78–1.71 (m, 2H), 1.55–1.19 (m, 48H), 0.99–0.85 (m, 24H). MS (MALDI-TOF): $m/z$ 969.65 $[MH]^+$.

*Synthesis of compound B-2TPIC*

To a dry three-necked round bottom flask were added compound **3** (97 mg, 0.10 mmol), IC2F (57 mg, 0.25 mmol), toluene (10 mL), acetic anhydride (0.5 mL) and $BF_3{\cdot}Et_2O$ (0.3 mL). The reaction mixture was stirred at room temperature for 30 min and then poured into methanol (50 mL). After filtered, the residue was purified by column chromatography on silica gel using petroleum ether: $CH_2Cl_2$ (2:1, v/v) as eluent yielding black solid (118 mg, 85%). $^1$H NMR (600 MHz, $CDCl_3$): $\delta$ 8.87 (s, 2H), 8.37 (s, 2H), 8.34 (s, 2H), 7.60 (s, 2H), 7.51 (s, 2H), 7.11 (s, 2H), 4.21–4.16 (m, 4H), 4.10–4.07 (m, 4H), 1.97–1.91 (m, 4H), 1.44–1.16 (m, 48H), 1.07–1.03 (m, 6H), 0.97–0.94 (m, 6H), 0.85–0.80 (m, 12H). $^{13}$C NMR (151 MHz, $CDCl_3$): $\delta$ 184.88, 160.17, 152.97, 151.54, 150.34, 135.98, 135.66, 134.74, 128.32, 128.04, 123.99, 119.24, 119.17, 115.90, 115.10, 114.44, 114.30, 112.07, 111.95, 109.75, 71.84, 66.16, 50.75, 39.97, 39.69, 31.72, 31.28, 31.01, 30.83, 29.63, 29.24, 28.50, 26.30, 24.31, 23.12, 23.00, 22.61, 14.15, 14.04, 13.97, 11.27. HR-MS (MALDI-TOF): $m/z$ 1393.70018 $[MH]^+$.

*Synthesis of compound **4***

To a dry three-necked round bottom flask were added 3,4-dimethoxythiophene (290 mg, 2.00 mmol), 2-ethylhexan-1-ol (1.04 g, 8.00 mmol), TsOH (35 mg, 0.20 mmol) and dry toluene (10 mL). After deoxygenated with argon for 30 min, the reaction mixture was stirred at 110 °C for 6 h. After cooling, the mixture was quenched with water and extracted with $CH_2Cl_2$ (30 mL × 3). The organic layer was dried over anhydrous $Na_2SO_4$ and filtered. After removing the solvent under reduced pressure, the

residue was purified by column chromatography on silica gel using petroleum ether: ethyl acetate (100:1, v/v) as eluent yielding colorless oil (612 mg, 90%). $^1$H NMR (400 MHz, $CDCl_3$): $\delta$ 6.16 (s, 2H), 3.84 (d, $J$ = 6.0 Hz, 4H), 1.75 (m, 2H), 1.50–1.31(m, 16H), 0.93 (m, 12H).

*Synthesis of compound **5***

To a dry three-necked round bottom flask was added a solution of compound **4** (510 mg, 1.50 mmol) in DMF (10 mL) at 0 °C. NBS (587 mg, 3.30 mmol) in DMF (5 mL) was added dropwise to the solution under darkness. The reaction mixture was stirred at room temperature for 16 h before being poured into water. After being extracted with $CH_2Cl_2$ (50 mL × 3), the organic layer was dried over anhydrous $Na_2SO_4$ and filtered. After removing the solvent under reduced pressure, the residue was purified by column chromatography on silica gel using petroleum ether: $CH_2Cl_2$ (50:1, v/v) as the eluent yielding colorless oil (605 mg, 81%). $^1$H NMR (400 MHz, $CDCl_3$): $\delta$ 3.94 (m, 4H), 1.29–1.65 (m, 18H), 0.93 (m, 12H).

*Synthesis of compound **6***

To a dry three-necked round flask was added compound **1** (0.33 M in toluene, 7.2 mL, 2.4 mmol), compound **5** (502 mg, 1.00 mmol) and dry toluene (10 mL). After deoxygenated with argon for 20 min, $Pd(PPh_3)_4$ (58 mg, 0.050 mmol) was added and then deoxygenated with argon for another 20 min. The reaction mixture was stirred at reflux for 24 h. After cooling, the mixture was extracted with $CH_2Cl_2$ (50 mL × 3) and the organic layer was dried over anhydrous $Na_2SO_4$ and filtered. After removing the solvent under reduced pressure, the residue was purified by column chromatography on silica gel using petroleum ether: $CH_2Cl_2$ (6:1, v/v) as the eluent yielding yellow oil (830 mg, 78%). $^1$H NMR (400 MHz, $CDCl_3$): $\delta$ 7.08 (s, 2H), 7.02 (s, 2H), 4.41 (m, 4H), 4.34 (m, 4H), 3.94 (m, 4H), 2.05–2.00 (m, 2H), 1.91–1.85 (m, 2H), 1.65–1.23 (m, 54H), 1.05–1.02 (m, 6H), 0.97–0.94 (m, 6H), 0.86–0.81 (m, 12H). MS (MALDI-TOF): $m/z$ 1063.66 $[MH]^+$.

*Synthesis of compound 7*

To a dry three-necked round bottom flask were added compound **6** (0.53 g, 0.50 mmol) and dry $CH_2Cl_2$ (10 mL). The mixture was deoxygenated with argon for 20 min. A solution of $LiAlH_4$ (1.0 M in THF, 1.42 mL, 1.42 mmol) was added dropwise at 0 °C. The mixture was stirred at 0 °C for 2 h. A saturated NaOH aqueous solution (10 mL) was added and the mixture was extracted with EtOAc (30 mL × 3). The organic layer was dried over anhydrous $Na_2SO_4$ and filtered. After removing the solvent, the residue was dissolved in $CHCl_3$ again, and $MnO_2$ (1.09 g, 1.25 mmol) was added in a dry three-necked round bottom flask under argon. The mixture was deoxygenated with argon for 20 min and was refluxed overnight. After cooling to room temperature, the reaction mixture was filtered through a pad of celite and the filtrate was dried over anhydrous $Na_2SO_4$ and filtered. After removing the solvent, the residue was purified by column chromatography on silica gel using petroleum ether: $CH_2Cl_2$ (2:1, v/v) as eluent yielding yellow solid (290 mg, 60%). $^1$H NMR (400 MHz, $CDCl_3$): $\delta$ 9.96 (s, 2H), 7.08 (s, 2H), 7.02 (s, 2H), 4.41 (m, 4H), 3.94 (m, 4H), 2.05–2.00 (m, 2H), 1.91–1.85 (m, 2H), 1.65–1.23 (m, 48H), 1.05–1.02 (m, 6H), 0.97–0.94 (m, 6H), 0.86–0.81 (m, 12H). MS (MALDI-TOF): *m*/*z* 975.61 $[MH]^+$.

*Synthesis of compound T-2TPIC*

To a dry three-necked round bottom flask were added compound **7** (120 mg, 0.12 mmol), IC2F (69 mg, 0.30 mmol), toluene (10 mL), acetic anhydride (0.5 mL) and $BF_3{\cdot}Et_2O$ (0.3 mL). The reaction mixture was stirred at room temperature for 30 min and then poured into methanol (50 mL). After filtered, the residue was purified by column chromatography on silica gel using petroleum ether: $CH_2Cl_2$ (2:1, v/v) as eluent yielding black solid (126 mg, 75%). $^1$H NMR (600 MHz, $CDCl_3$): $\delta$ 8.92 (s, 2H), 8.38 (s, 2H), 8.32 (s, 2H), 7.59 (s, 2H), 6.85 (s, 2H), 4.14–4.08 (m, 8H), 2.05–2.00 (m, 2H), 1.91–1.85 (m, 2H), 1.44–1.14 (m, 48H), 1.05–1.02 (m, 6H), 0.97–0.94 (m, 6H), 0.86–0.81 (m, 12H). $^{13}$C NMR (151 MHz, $CDCl_3$): $\delta$ 184.84, 159.97, 154.97, 154.79, 153.07, 151.80, 148.74, 145.57, 135.97, 134.73, 128.87, 127.85, 121.12, 119.40, 119.23, 115.75,

115.03, 114.43, 114.28, 112.19, 112.07, 105.07, 66.36, 50.65, 40.43, 39.81, 31.74, 31.09, 30.86, 30.19, 29.58, 29.10, 28.41, 26.18, 23.60, 23.18, 23.00, 22.63, 14.14, 14.09, 13.99, 11.12. HR-MS (MALDI-TOF): *m*/*z* 1399.65542 $[MH]^+$.

**Characterizations**

The $^1H$ and $^{13}C$ NMR spectra were measured on Bruker AVANCE 400 MHz and 600 MHz spectrometers. Mass spectra were measured on a Bruker Daltonics BIFLEX III MALDI-TOF Analyzer using MALDI mode. Solution (chloroform) and thin film (on quartz substrate) UV-vis absorption spectra were recorded on a JΛSCO V-570 spectrophotometer. The steady-state photoluminescence and time-resolved photoluminescence spectra of films were measured using an FLS1000 spectrometer. The films were prepared by spin-coating the solution (15 mg $mL^{-1}$ in chloroform) at 2000 rpm for 40 s on the quartz substrate.

Electrochemical measurements were carried out under nitrogen on a deoxygenated solution of tetra-*n*-butylammonium hexafluorophosphate (0.1 M) in $CH_3CN$ using a computer-controlled CHI660C electrochemical workstation, a glassy-carbon working electrode, a platinum-wire auxiliary electrode, and an Ag/AgCl as a reference electrode. The samples were first dissolved in chloroform, and the resulting solutions were drop-cast onto a glassy carbon working electrode to form thin films prior to the measurements. Potentials were referenced to ferrocenium/ferrocene ($FeCp_2^{0/+}$) couple by using ferrocene as an internal standard. The HOMO and LUMO energy levels of the samples were estimated from onset redox potentials, assuming the absolute energy level of $FeCp_2^{0/+}$ to be 4.8 eV below vacuum. The HOMO and LUMO energy levels of the samples were calculated as:

$$E_{HOMO} = -(E_{ox}^{onset} + 4.8\ eV) \quad \text{eqn S1}$$

$$E_{LUMO} = -(E_{red}^{onset} + 4.8\ eV) \quad \text{eqn S2}$$

where $E_{ox}^{onset}$ (onset potentials for oxidation) and $E_{red}^{onset}$ (onset potentials for reduction) are defined as the difference between the respective onset potential of the sample and the redox potential of $FeCp_2^{0/+}$.

Grazing incidence wide-angle X-ray scattering (GIWAXS) measurements were accomplished with a Xeuss 2.0 SAXS/WAXS laboratory beamline using a Cu X-ray source (8.05 keV, 1.54 Å) and a Pilatus3R 300K detector. The incidence angle is 0.2º. GIWAXS samples were prepared by spin coating B-2TPIC or T-2TPIC chloroform solution (12 mg $mL^{-1}$) at 1500 rpm for 40 s on silicon substrate.

The hydrodynamic diameter and the zeta potentials of nanoparticles were measured by dynamic light scattering (Malvern Zetasizer ZS).

**Computational methodology**

Density functional theory (DFT) calculations were carried out at the B3LYP/6-31G(d) level in the Gaussian 16 package,[S3] where all alkyl side chains of B-2TPIC and T-2TPIC were replaced by methyl groups to simplify the calculations. Geometry optimizations were performed with full relaxation of all atoms in gas phase, following which vibration frequency calculations were used to check that the optimized structures had no imaginary frequency. Charge distribution of the molecules was examined by Mulliken population analysis. The surface electrostatic potential (ESP) mapping was obtained by using the Multiwfn software.[S4, S5]

**SCLC measurements**

Hole-only devices were fabricated for hole mobility measurements with the structure of ITO/PEDOT:PSS/active layer/$MoO_3$/Ag. The ITO substrates were first scrubbed by detergent and then sonicated with deionized water, acetone and isopropanol subsequently, and dried in an oven. The ITO glass substrates were treated by UV-ozone for 20 min before use. PEDOT:PSS was spin-coated onto the ITO substrates at 4000 rpm for 30 s. After annealing at 150 °C for 15 min in air, the active layers were formed by spin-coating a solution of B-2TPIC or T-2TPIC (18 mg $mL^{-1}$ in chloroform) at 2000 rpm for 40 s on PEDOT:PSS in a glovebox. Then, the $MoO_3$ layer (ca. 5 nm) and Ag (ca. 90 nm) were successively evaporated onto the surface of the photoactive layer under vacuum (ca. $10^{-5}$ Pa).

Electron-only devices were fabricated for electron mobility measurements with the structure ITO/ZnO/active layer/PDINN/Ag. The mixture of zinc acetate dihydrate (100 mg), 2-methoxyethanol (973 μL) and ethanolamine (28.29 μL) was stirred overnight to prepare the ZnO precursor solution. After the pretreatment of the ITO substrate, ZnO layer (ca. 30 nm) was spin-coated onto the ITO substrate at 4000 rpm for 30 s from ZnO precursor solution. After annealing at 200 °C for 30 min, the active layers were formed by spin-coating a solution of B-2TPIC or T-2TPIC (18 mg $mL^{-1}$ in chloroform) at 2000 rpm for 40 s on ZnO in a glovebox. Then, a thin PDINN layer (~ 5 nm) was coated on the active layer, followed by the deposition of Ag electrode (90 nm).

The active area of the device was 4 $mm^2$ and the thickness of the active layer was 90 nm. The mobility was extracted by fitting the *J–V* curves using space charge limited current (SCLC) method: [S6]

$$J=\frac{9\varepsilon_r\varepsilon_0\mu V^2}{8L^3} \quad \text{---------- eqn S3}$$

here, $J$ refers to the current density, $\mu$ is hole or electron mobility, $\varepsilon_r$ is relative dielectric constant of the transport medium, which is equal to 3, $\varepsilon_0$ is the permittivity of free space ($8.85 \times 10^{-12}$ F $m^{-1}$), $V = V_{appl} - V_{bi}$, where $V_{appl}$ is the applied voltage to the device, and $V_{bi}$ is the built-in voltage due to the difference in work function of the two electrodes, $L$ is the thickness of the active layer.

**Nanoparticle preparation**

Individual stock solutions (0.5 mg $mL^{-1}$) of B-2TPIC, T-2TPIC and PM6 were prepared in chloroform. The solutions were stirred at room temperature for 2 h. The precursor solutions of single-component nanoparticles (NPs) were prepared with the corresponding stock solution, while that of heterojunction NPs were prepared from the stock solutions by mixing them in the ratio of the desired NP composition. Then NP precursor solution (1 mL) was added to the different weight ratios of TEBS aqueous solution (4 mL) and then sonicated for 5 min with an ultrasonic processor (Sonics SCIENTZ-IID) to obtain the mini-emulsion. The mini-emulsion was evaporated to remove the chloroform, obtaining a surfactant-stabilized NP dispersion in water. Finally,

the dispersion was filtered (0.45-μm mixed cellulose) to remove any large aggregates. The final composition was determined by the following: 2 mL methanol was added to 1 mL samples for de-emulsification. Then 2 mL chloroform was added to extract the semiconductor material dissolved in chloroform. The solution was evaporated to remove the organic solvents and then 1 mL chloroform was added to the samples. Finally, the solution was measured by UV-vis absorption to determine the final weight of B-2TPIC, T-2TPIC, PM6:B-2TPIC or PM6:T-2TPIC NPs in the solutions.

**Hydrogen evolution**

The concentration of single-component (B-2TPIC or T-2TPIC) NPs and heterojunction (PM6:B-2TPIC or PM6:T-2TPIC) NPs was calibrated by UV-vis absorption. Then, different volumes of photocatalyst NPs solution were added to the prepared ascorbic acid (AA) aqueous solution (0.2 M) to obtain NPs solutions with different concentrations, and the total volume was maintained at 7.5 mL. The concentration of the suspensions with single-component (B-2TPIC or T-2TPIC) NPs and heterojunction (PM6:B-2TPIC or PM6:T-2TPIC) NPs for the HER was 6.67 μg $mL^{-1}$ or 26.67 μg $mL^{-1}$. According to the usage for corresponding reaction condition, a certain amount of $K_2PtCl_6$ aqueous solution (1 mg $mL^{-1}$) was added to the above-mentioned NPs solutions with corresponding concentrations. The aging treatment of the $K_2PtCl_6$ solution was performed according to the modified method reported in literature,[S7] and different aging treatments affect the initial demand for Pt loading ratios. For the HER under simulated solar light illumination (AM 1.5G, 100 mW $cm^{-2}$), the mixed reaction solution was added into a recirculating batch reactor (cross sectional area, 5.786 $cm^2$; penetration depth of light, 1.296 cm) kept at 5 °C. The recirculating batch reactor was purged with nitrogen several times to remove oxygen, and the pressure was set to 1.2 kPa. The suspensions with photocatalyst NPs were stirred and illuminated with a 300 W Xe lamp equipped with a mirror module (330−1100 nm) and AM 1.5G filtered. Multiple-channel reactors were applied to improve the efficiency of screening the hydrogen evolution conditions of single-component (B-2TPIC or T-

2TPIC) NPs and heterojunction (PM6:B-2TPIC or PM6:T-2TPIC) NPs. The photocatalyst NPs formed under various conditions were respectively added into each off-line reactors (cross-sectional area, 3.142 $cm^2$; penetration depth of light, 2.387 cm) with 0.2 M AA in aqueous solution (7.5 mL), and then the reactors were purged with nitrogen several times to remove oxygen. The suspensions with photocatalyst NPs were stirred at room temperature and illuminated with the light source which covered the visible range (400−800 nm, 100 mW $cm^{-2}$). All hydrogen evolution was evaluated by an all-glass automatic online trace gas analysis system (Labsolar 6A, PerfectLight) with an online gas chromatograph (Thermal conductivity detector, $N_2$ carrier). The multiple-channel photochemical reaction system is configured with an LED lamp (400−800 nm, 100 mW $cm^{-2}$) rather than the reference spectrum for standard tests of solar energy conversion systems (AM 1.5G, 100 mW $cm^{-2}$). Meanwhile, the reactor has a light-concentrating effect leading to the actual irradiation intensity being higher than 100 mW $cm^{-2}$. Hence, all values from multiple-channel reactors are normalized to the maximum value in each set of parallel experiments to obtain the optimal conditions. Three parallel hydrogen evolution experiments of the champion PM6:B-2TPIC NPs were conducted under the same optimized conditions to verify reproducibility.

**EQE measurements**

EQE was measured by using PM6:B-2TPIC (26.67 μg $mL^{-1}$; D:A, 4:6, w/w; 0.3 wt% TEBS/$H_2O$; 20 wt% Pt loading) or PM6:T-2TPIC (26.67 μg $mL^{-1}$; D:A, 3:7, w/w; 0.5 wt% TEBS/$H_2O$; 16 wt% Pt loading) and 0.2 M AA aqueous solution (7.5 mL; cross-sectional area, 5.786 $cm^2$; penetration depth of light, 1.3 cm). An all-glass automatic online trace gas analysis system (Labsolar 6A, PLS-SXE300+, PerfectLight) was used for the measurements, equipped with an online gas chromatograph featuring a thermal conductivity detector and $N_2$ as the carrier gas. Monochromatic light (400 nm, 500 nm, 600 nm, 700 nm, 808 nm) was obtained from a 300 W xenon lamp fitted with corresponding bandpass filters which have a bandwidth of 15 nm. The sample was first illuminated under AM 1.5G light, 100 mW $cm^{-2}$ for 2 h to complete Pt photodeposition.

Then, the reactor was evacuated to remove all of the $H_2$ that evolved during this time. The light source was fitted with a corresponding bandpass filter for EQE measurements. The EQE was calculated using equations:[S8]

$$\mathrm{EQE} = 2 \times \frac{n_\mathrm{h}}{n_\mathrm{p}} \quad \text{---------- eqn S4}$$

$$n_\mathrm{p} = \frac{It\lambda}{N_A hc} \quad \text{---------- eqn S5}$$

where $n_\mathrm{h}$ represents the number of moles of $H_2$ evolved per hour, $n_\mathrm{p}$ represents the total number of incident photons per hour, $I$ is the radiant power, $t$ is the irradiation time (excluding the induction time), $\lambda$ is the light wavelength, $N_\mathrm{A}$ is the Avogadro constant, $h$ is the Planck constant, $c$ is the speed of light.

**Transmission electron microscope (TEM)**

High-resolution field emission TEM (Hitachi HT7700) was employed to investigate the internal morphology of the PM6:B-2TPIC and PM6:T-2TPIC NPs. The fabrication of NPs for TEM measurements was described in nanoparticle preparation part. The specimen was prepared by placing 3.5 μL of solution onto the copper TEM grid and drying at room temperature. The TEM analysis was performed by setting the microscope at an acceleration voltage of 100 kV.

**Transient absorption**

Transient absorption (TA) data were collected by using a pump and probe femtosecond TA spectroscopy system (Vitara T-Legend Elite-TOPAS-Helios-EOS-Omni). The samples were prepared as described in nanoparticle preparation part with a concentration of 50 μg $mL^{-1}$, ensuring strong absorption when excited by a pump laser at 750 nm. Light in the ranges of 400−800 nm was served as the probe source.

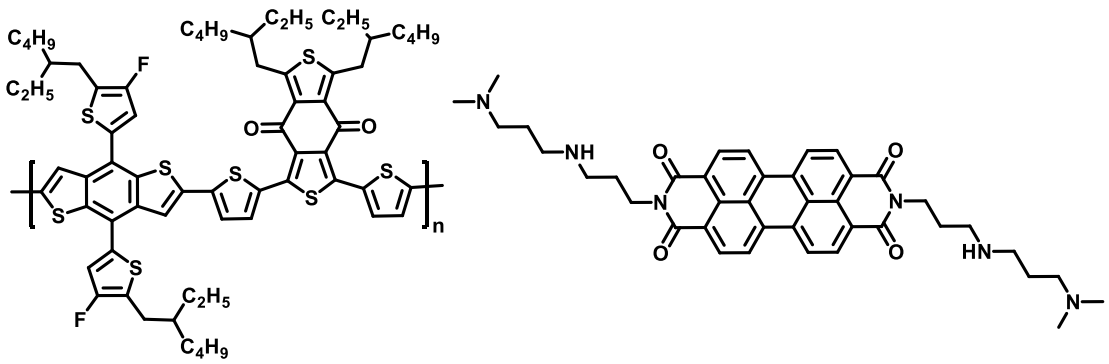

PM6 PDINN

**Fig. S1** Chemical structures of PM6 and PDINN.

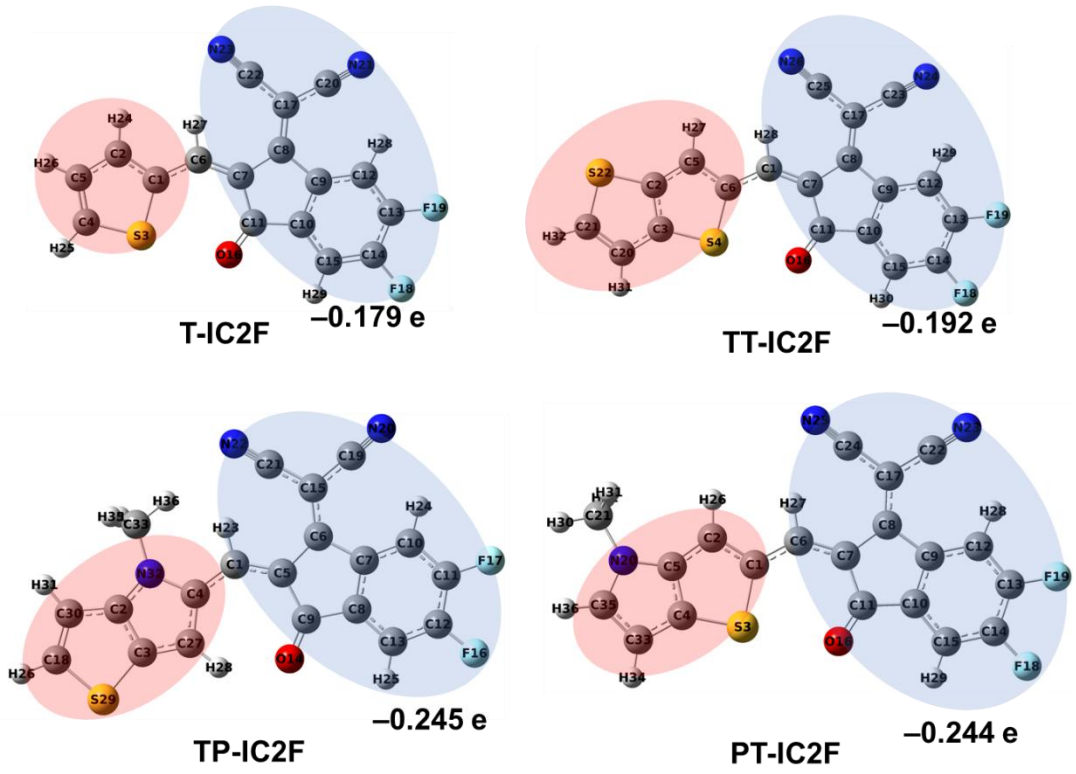


**Fig. S2** Mulliken population analysis of T-IC2F, TT-IC2F, TP-IC2F, and PT-IC2F.

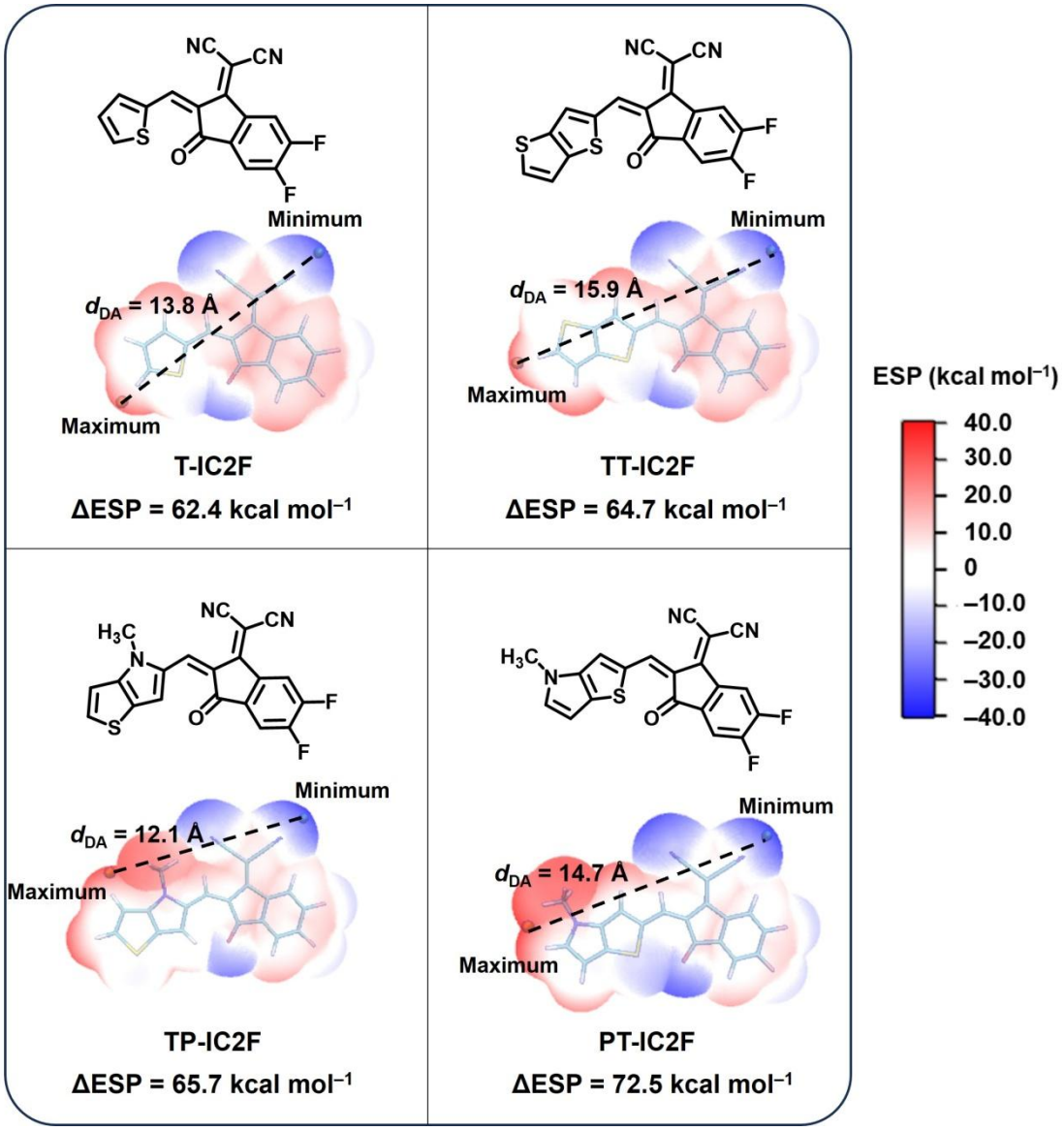


**Fig. S3** Chemical structures and surface ESP of T-IC2F, TT-IC2F, TP-IC2F, and PT-IC2F. In ESP diagrams, the orange spheres represent the surface maximum points, and the blue spheres represent the surface minimum points.

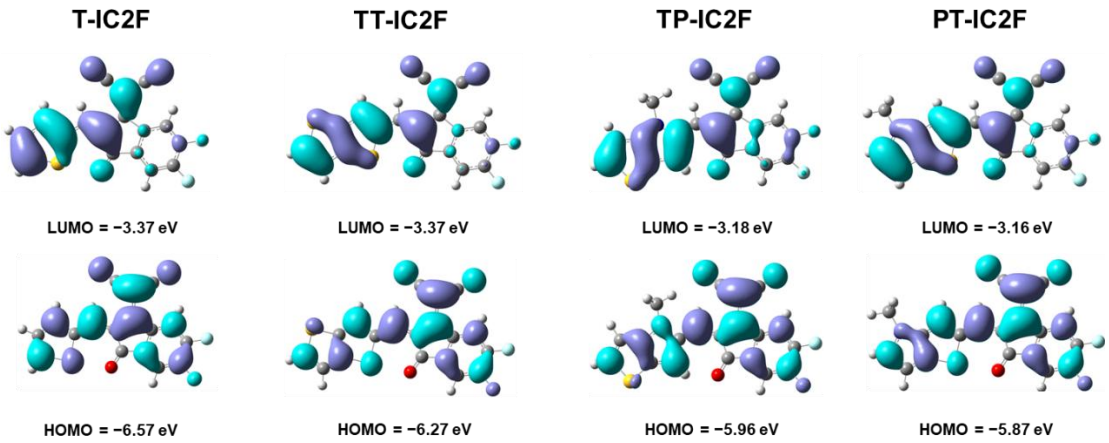


**Fig. S4** The energy levels of T-IC2F, TT-IC2F, TP-IC2F and PT-IC2F. Calculated at the B3LYP/6-31G(d) level (isovalue = 0.02).

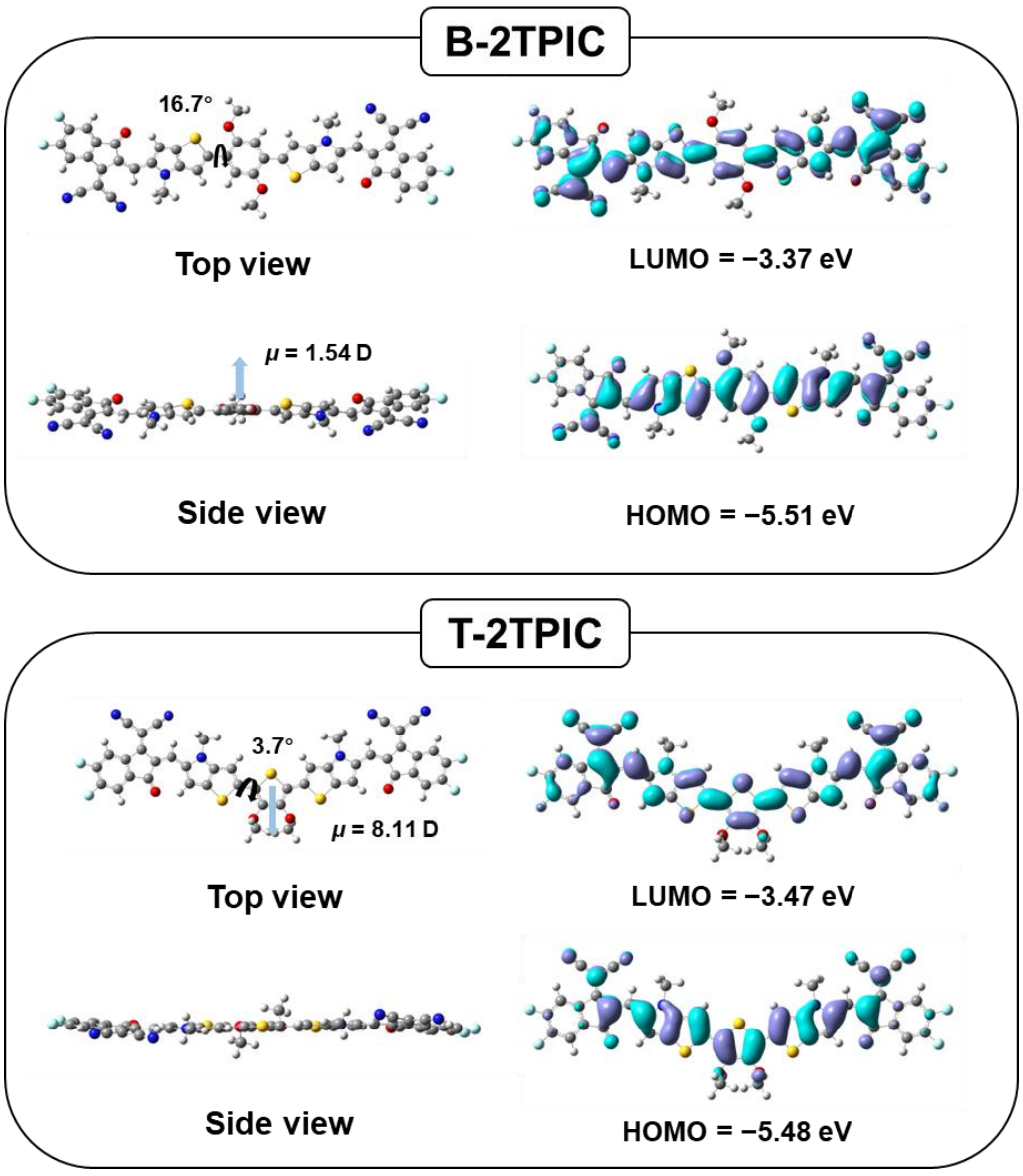


**Fig. S5** The optimized geometry and calculated energy levels of B-2TPIC and T-2TPIC at the B3LYP/6-31G(d) level. To simplify the calculation process, the alkyl side chains were replaced by methyl groups.

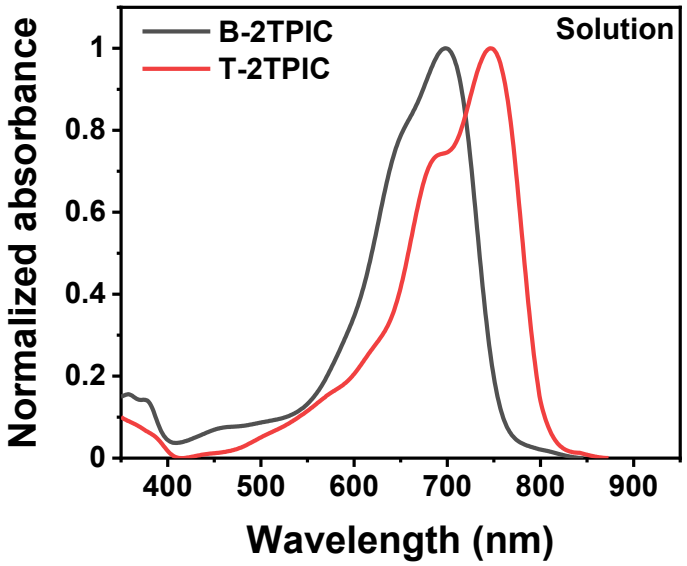


**Fig. S6** Normalized absorption spectra of B-2TPIC and T-2TPIC in chloroform solutions ($10^{-6}$ M).

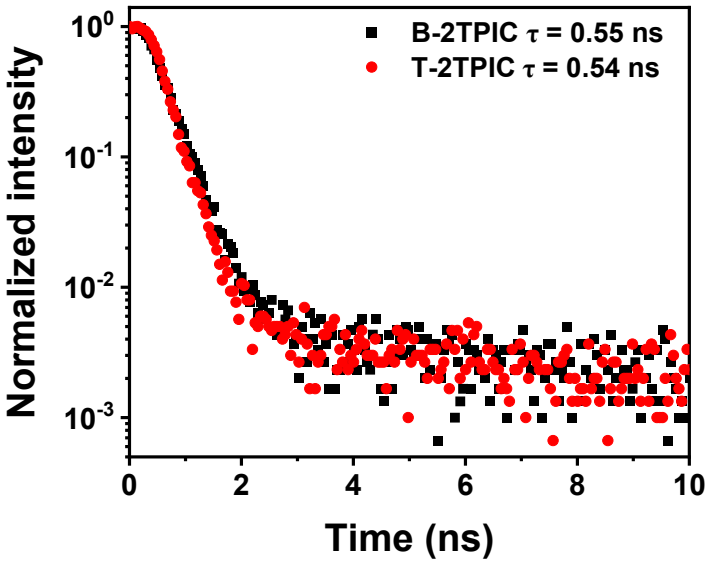


**Fig. S7** TRPL spectra of B-2TPIC and T-2TPIC in films.

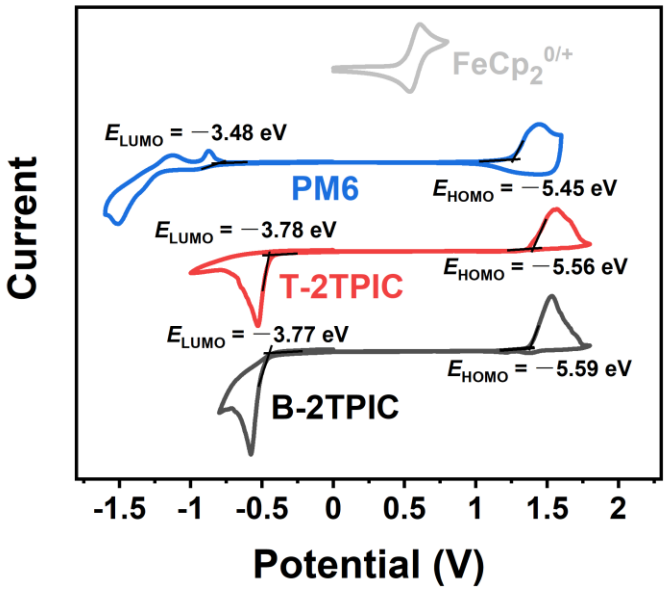


**Fig. S8** Cyclic voltammograms of B-2TPIC, T-2TPIC and PM6 in $CH_3CN$/0.1 M $[Bu_4N]^+[PF_6]^-$ at 100 mV $s^{-1}$, in which the horizontal scale refers to an Ag/AgCl electrode.

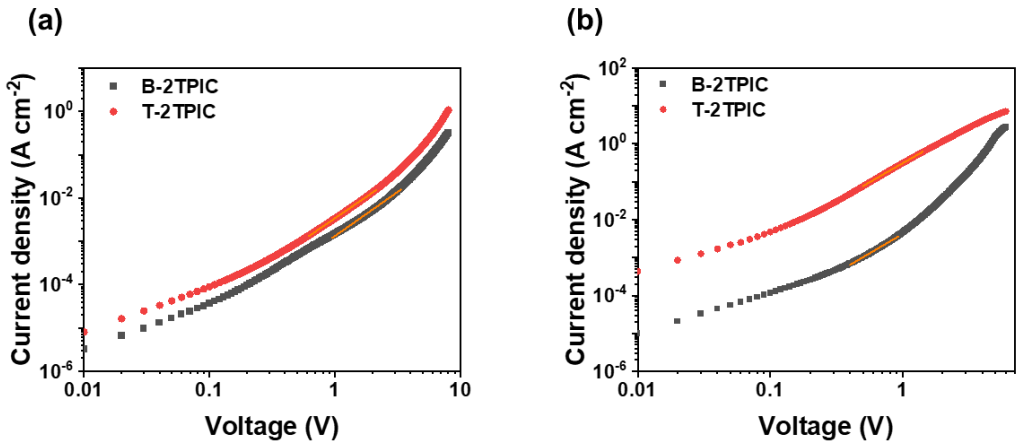


**Fig. S9** *J*–*V* characteristics in dark for (a) hole-only and (b) electron-only devices based on B-2TPIC and T-2TPIC.

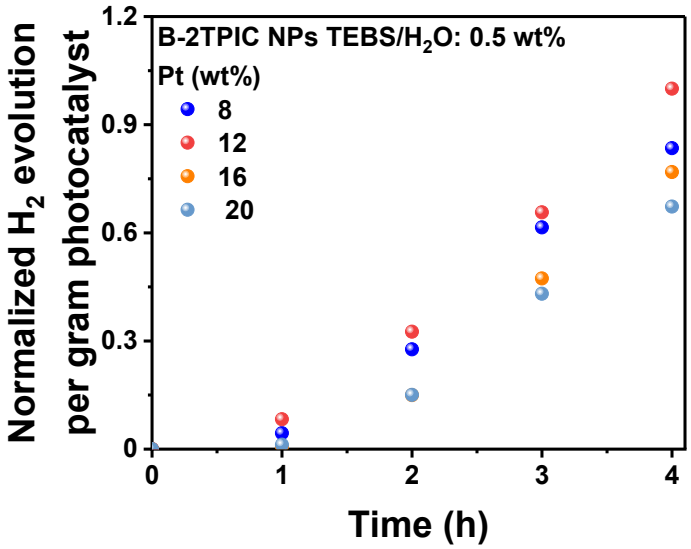


**Fig. S10** Normalized hydrogen evolution per gram photocatalyst versus time of B-2TPIC NPs at a concentration of 6.67 μg $mL^{-1}$ with 0.5 wt% TEBS/$H_2O$ and varying Pt loadings at room temperature, measured by a multiple-channel photochemical reaction system.

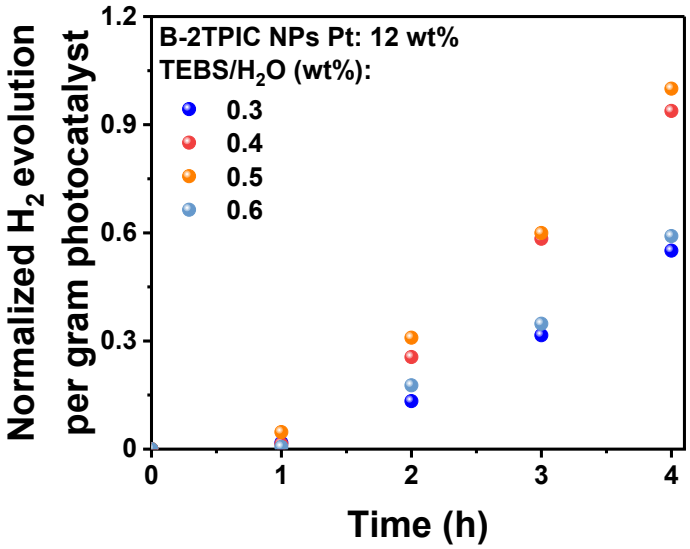


**Fig. S11** Normalized hydrogen evolution per gram photocatalyst versus time of B-2TPIC NPs at a concentration of 6.67 μg $mL^{-1}$ with 12 wt% Pt loading at different weight ratios of surfactant (TEBS/$H_2O$) at room temperature, measured by a multiple-channel photochemical reaction system.

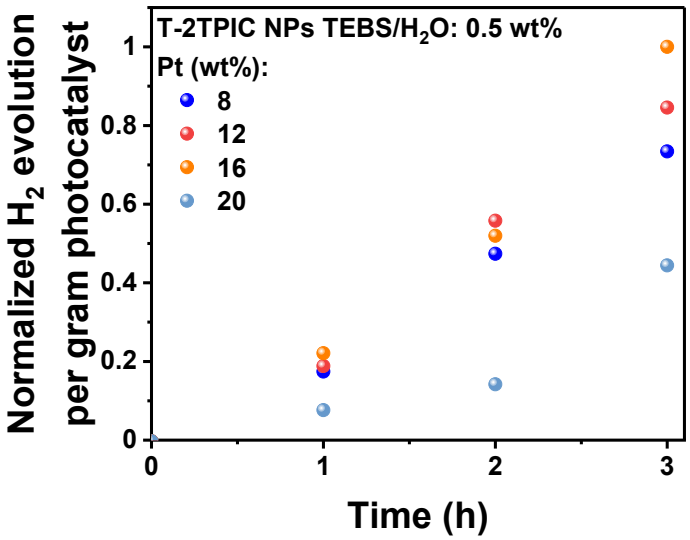


**Fig. S12** Normalized hydrogen evolution per gram photocatalyst versus time of T-2TPIC NPs at a concentration of 6.67 μg $mL^{-1}$ with 0.5 wt% TEBS/$H_2O$ and varying Pt loadings at room temperature, measured by a multiple-channel photochemical reaction system.

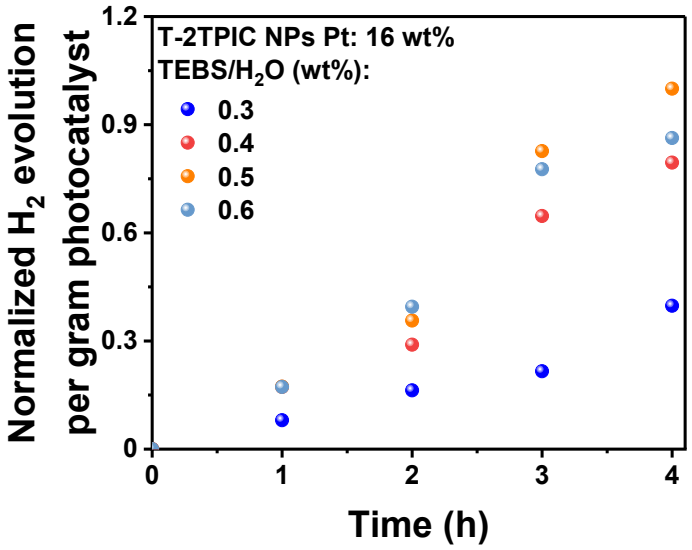


**Fig. S13** Normalized hydrogen evolution per gram photocatalyst versus time of T-2TPIC NPs at a concentration of 6.67 μg $mL^{-1}$ with 16 wt% Pt loading at different weight ratios of TEBS/$H_2O$ at room temperature, measured by a multiple-channel photochemical reaction system.

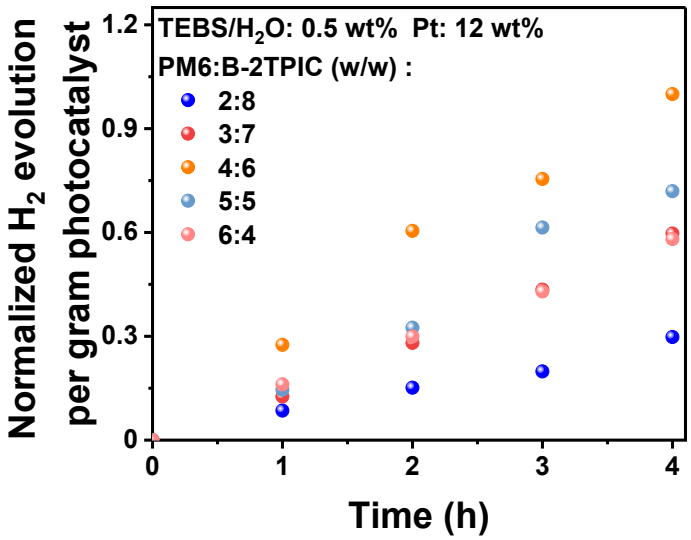


**Fig. S14** Normalized hydrogen evolution per gram photocatalyst versus time of nanoparticles formed with different PM6:B-2TPIC weight ratios using 0.5 wt% TEBS/$H_2O$ with 12 wt% Pt loading at a concentration of 6.67 μg $mL^{-1}$ at room temperature, measured by a multiple-channel photochemical reaction system.

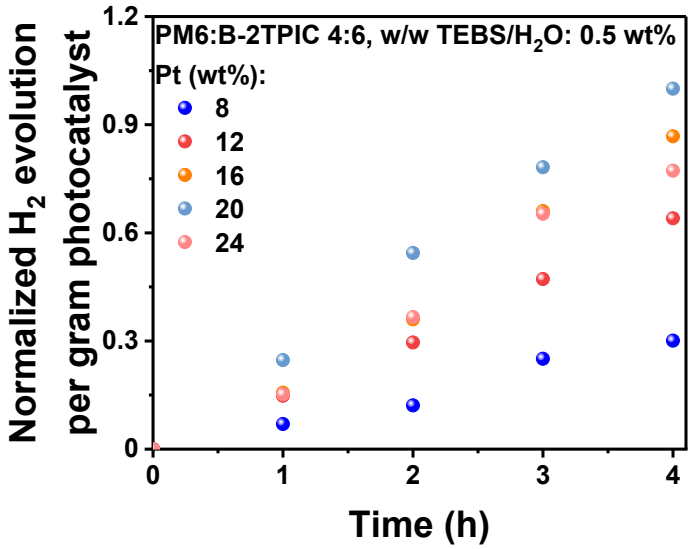


**Fig. S15** Normalized hydrogen evolution per gram photocatalyst versus time of PM6:B-2TPIC (4:6, w/w) NPs photocatalysts at a concentration of 6.67 μg $mL^{-1}$ with 0.5 wt% TEBS/$H_2O$ and varying Pt loadings at room temperature, measured by a multiple-channel photochemical reaction system.

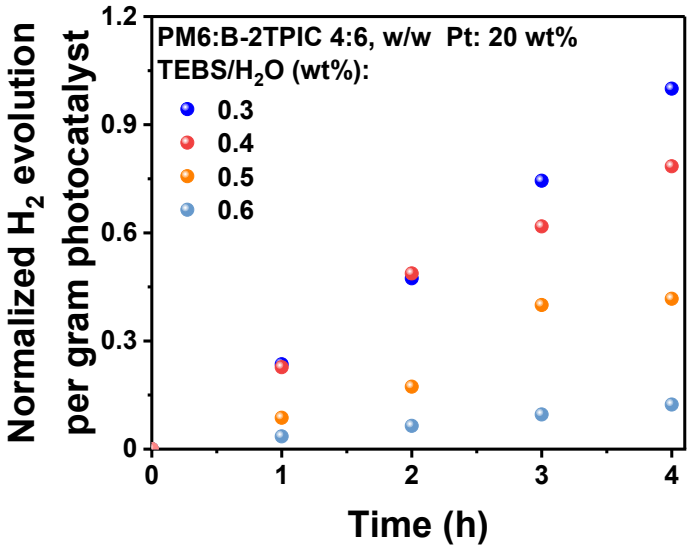


**Fig. S16** Normalized hydrogen evolution per gram photocatalyst versus time of PM6:B-2TPIC (4:6, w/w) NPs photocatalysts at a concentration of 6.67 μg $mL^{-1}$ with 20 wt% Pt loading at different weight ratios of TEBS/$H_2O$ at room temperature, measured by a multiple-channel photochemical reaction system.

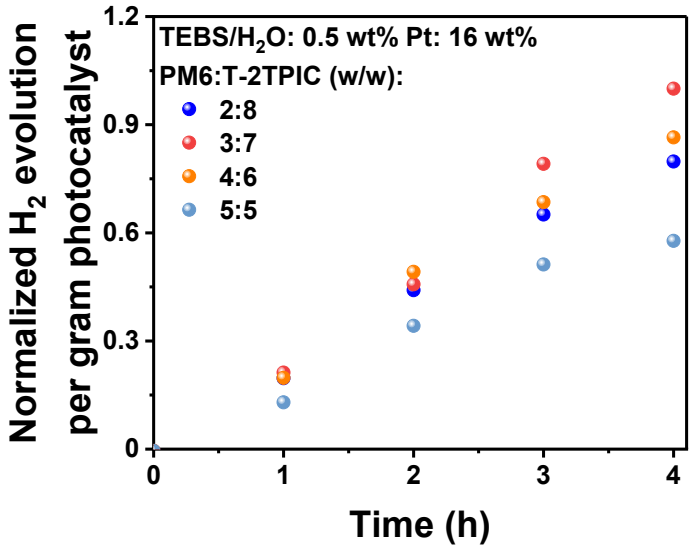


**Fig. S17** Normalized hydrogen evolution per gram photocatalyst versus time of nanoparticles formed with different PM6:T-2TPIC weight ratios using 0.5 wt% TEBS/$H_2O$ with 16 wt% Pt loading at a concentration of 6.67 μg $mL^{-1}$ at room temperature, measured by a multiple-channel photochemical reaction system.

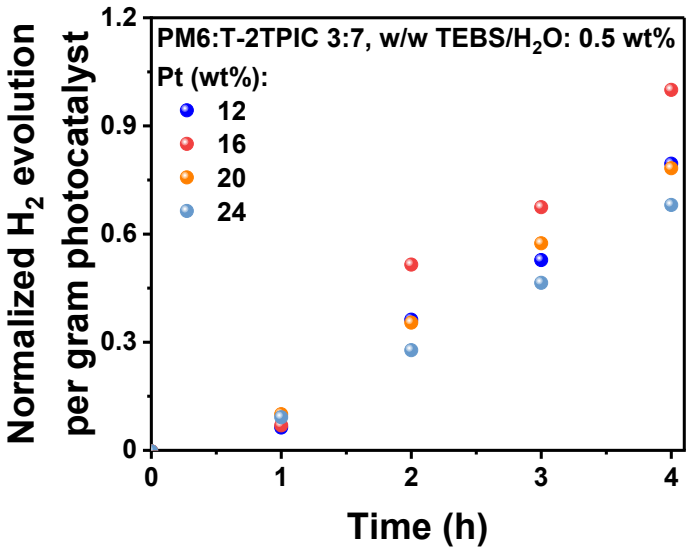


**Fig. S18** Normalized hydrogen evolution per gram photocatalyst versus time of PM6:T-2TPIC (3:7, w/w) NPs photocatalysts at a concentration of 6.67 μg $mL^{-1}$ with 0.5 wt% TEBS/$H_2O$ and varying Pt loadings at room temperature, measured by a multiple-channel photochemical reaction system.

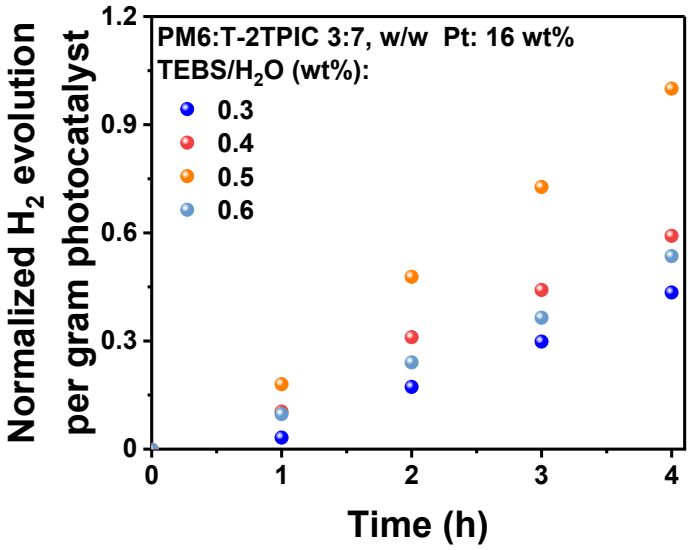


**Fig. S19** Normalized hydrogen evolution per gram photocatalyst versus time of PM6:T-2TPIC (3:7, w/w) NPs photocatalysts at a concentration of 6.67 μg $mL^{-1}$ with 16 wt% Pt loading at different weight ratios of TEBS/$H_2O$ at room temperature, measured by a multiple-channel photochemical reaction system.

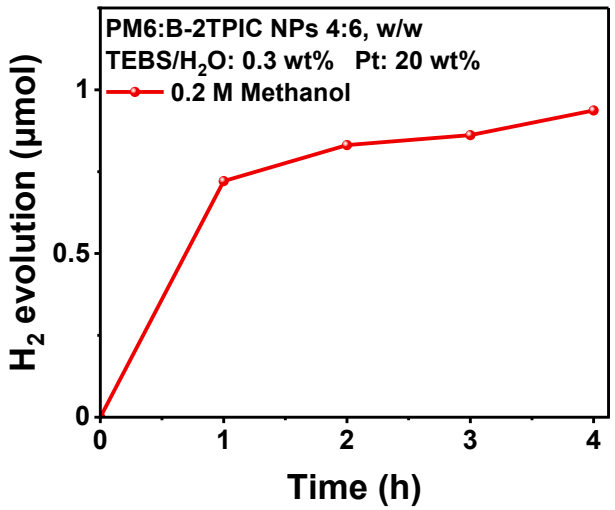


**Fig. S20** Hydrogen evolution versus time of PM6:B-2TPIC NPs (D:A ratio: 4:6, w/w, 0.3 wt% TEBS/$H_2O$ weight ratio and 20 wt% Pt loading) using methanol as the sacrificial agent at a concentration of 6.67 μg $mL^{-1}$, under AM 1.5G, 100 mW $cm^{-2}$.

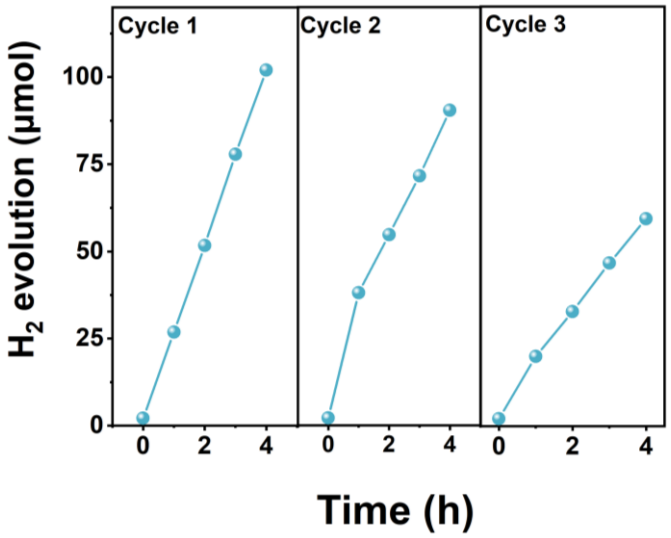


**Fig. S21** Cycling stability of PM6:B-2TPIC NPs (D:A ratio: 4:6, w/w, 0.3 wt% TEBS/$H_2O$ weight ratio and 20 wt% Pt loading) in 0.2 M AA at a concentration of 26.67 μg $mL^{-1}$, under AM 1.5G, 100 mW $cm^{-2}$. For recycling experiments, the equivalent amount of ascorbic acid was added after the end of every cycle, according to the consumption of ascorbic acid.

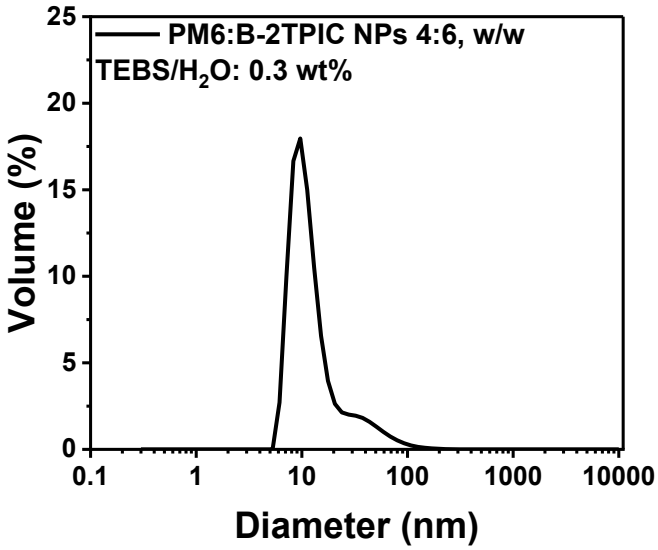


**Fig. S22** DLS size distributions by volume of PM6:B-2TPIC (4:6, w/w) NPs using 0.3 wt% TEBS/$H_2O$.

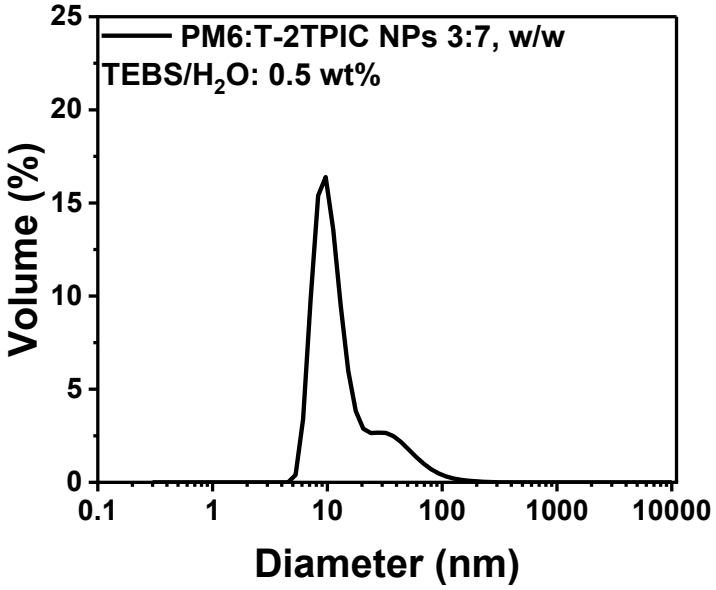


**Fig. S23** DLS size distributions by volume of PM6:T-2TPIC (3:7, w/w) NPs using 0.5 wt% TEBS/$H_2O$.

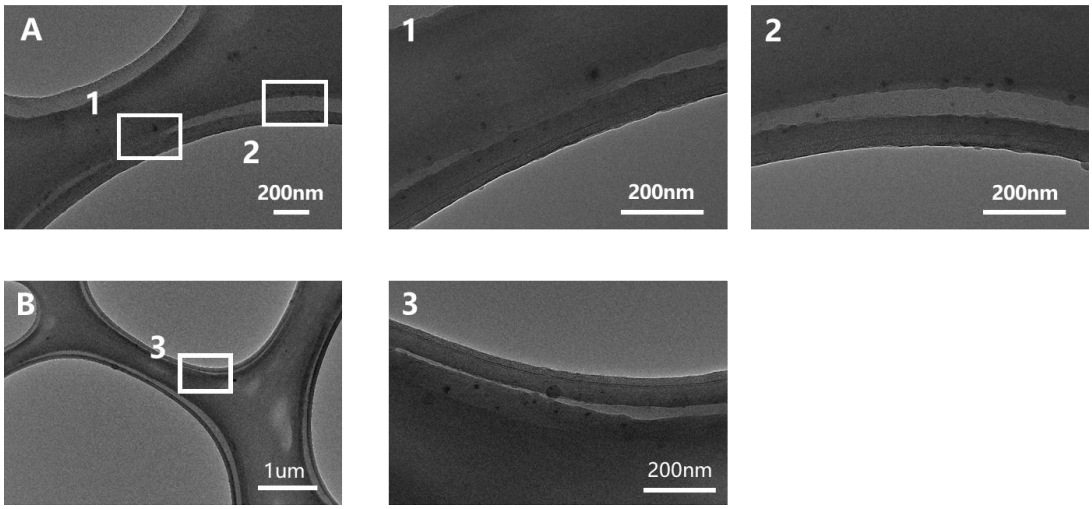


**Fig. S24** TEM images of PM6:B-2TPIC (4:6, w/w) NPs using 0.3 wt% TEBS/$H_2O$.

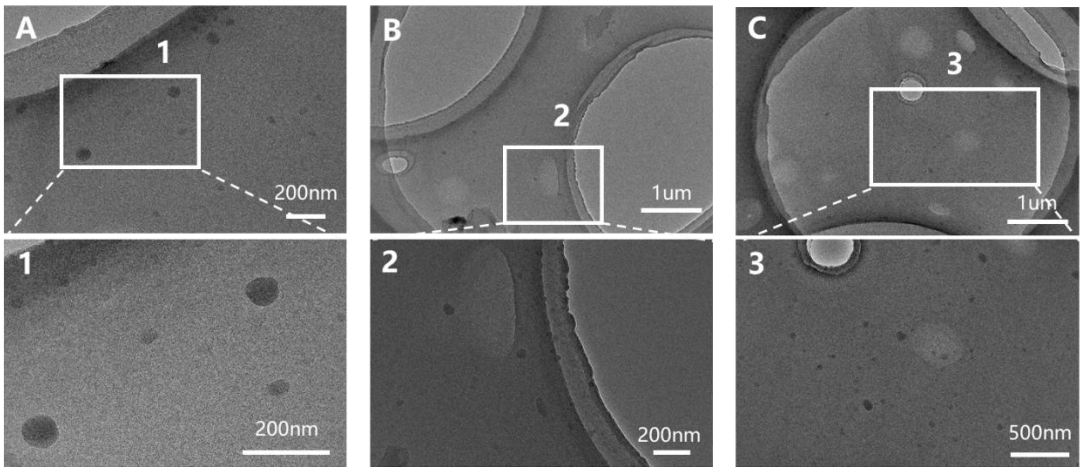


**Fig. S25** TEM images of PM6:T-2TPIC (3:7, w/w) NPs using 0.5 wt% TEBS/$H_2O$.

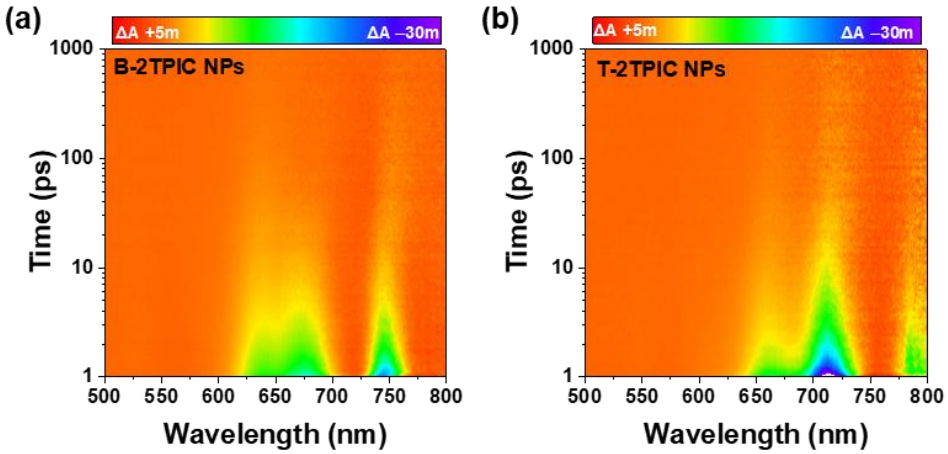


**Fig. S26** The 2D transient absorption contours in the 500–800 nm range of (a) B-2TPIC and (b) T-2TPIC NPs. Excited at 750 nm.

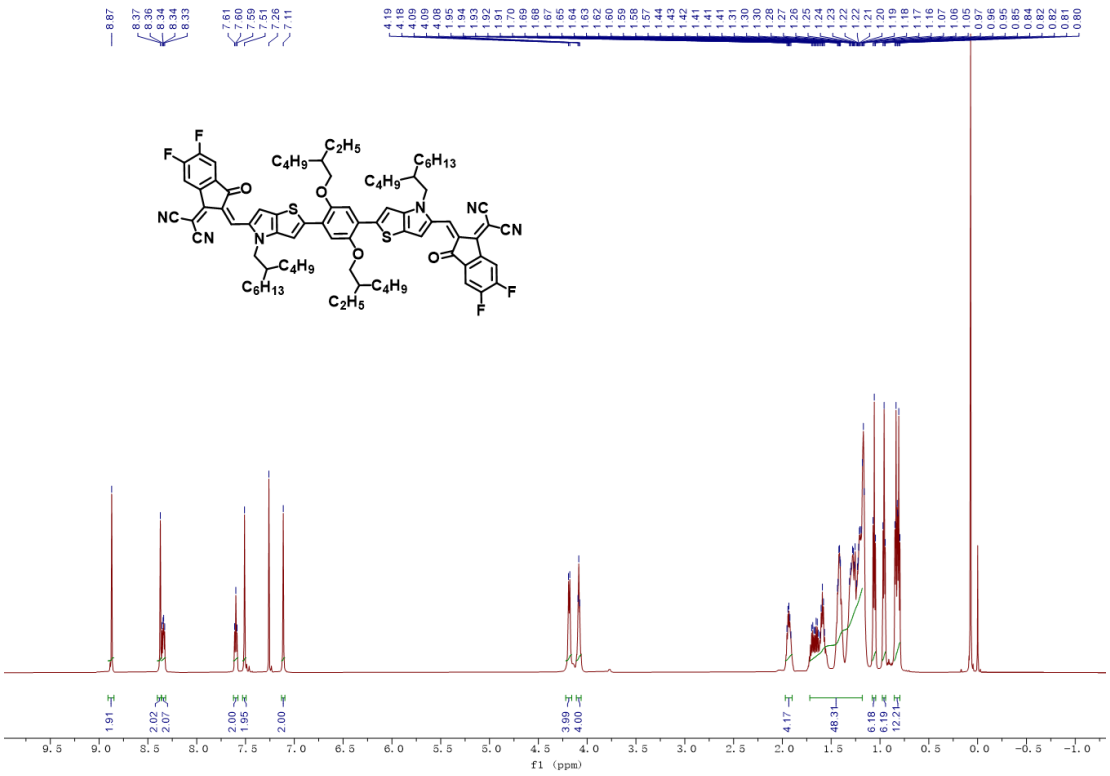


**Fig. S27** $^{1}$H NMR Spectrum of B-2TPIC.

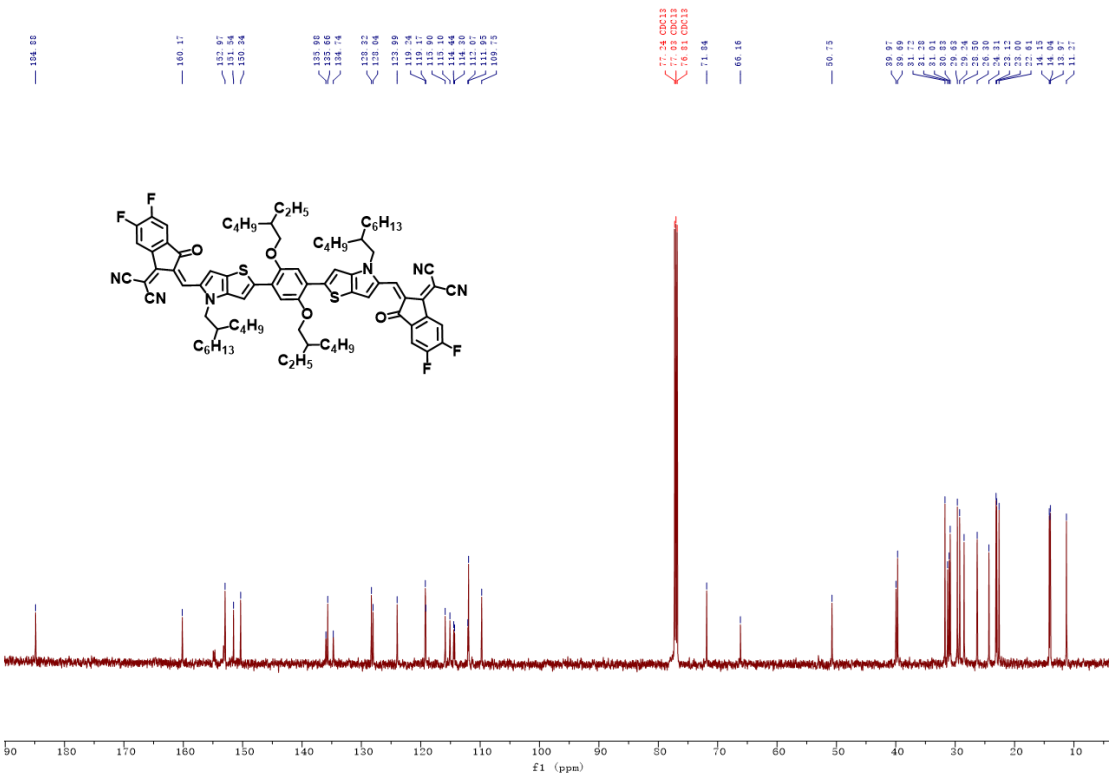


**Fig. S28** $^{13}$C NMR Spectrum of B-2TPIC.

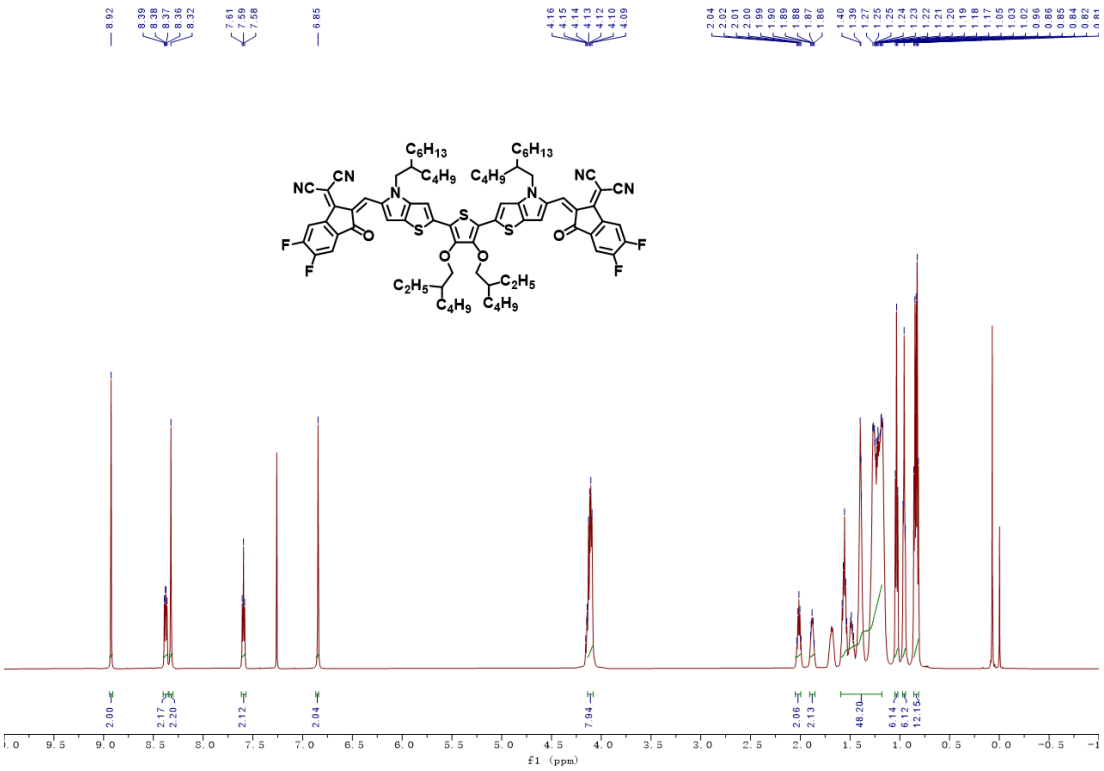


**Fig. S29** $^{1}$H NMR Spectrum of T-2TPIC.

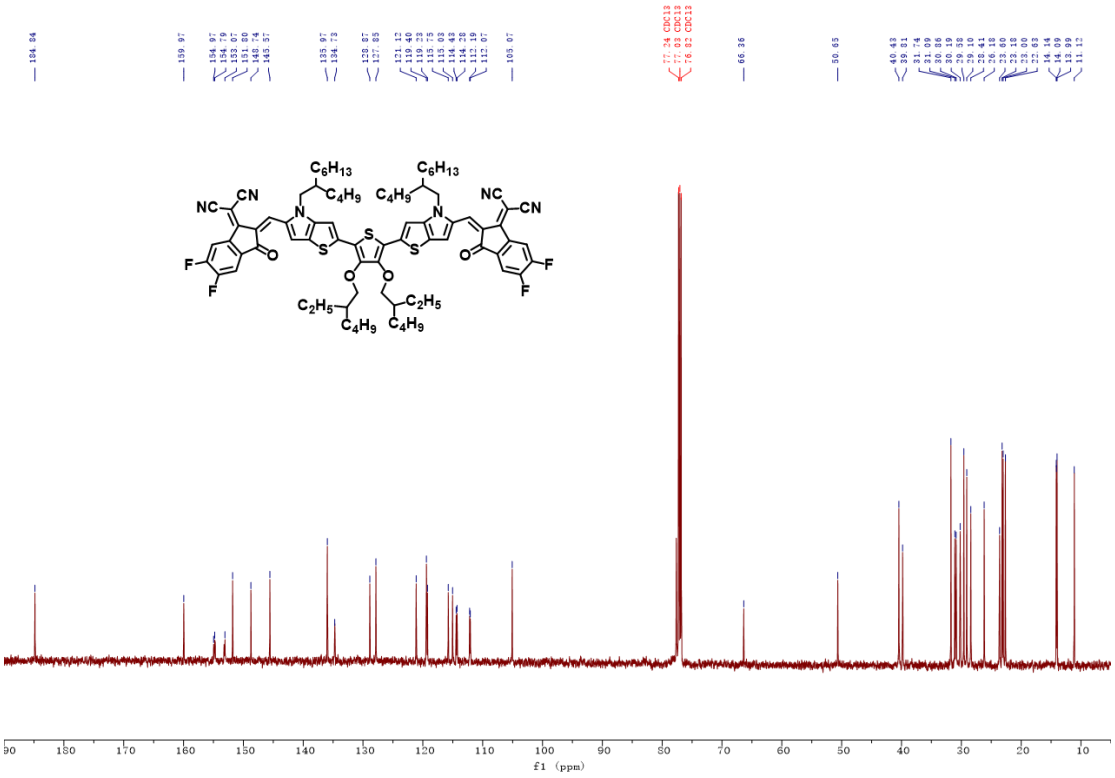


**Fig. S30** $^{13}$C NMR Spectrum of T-2TPIC.

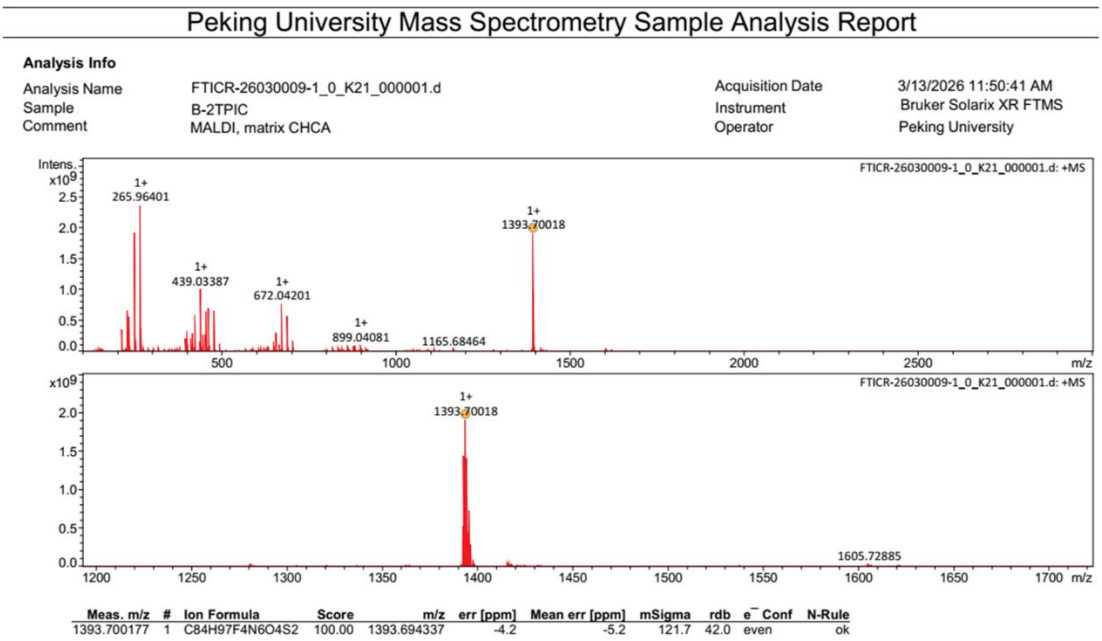


**Fig. S31** HR mass spectrum of B-2TPIC using the MALDI-TOF mode.

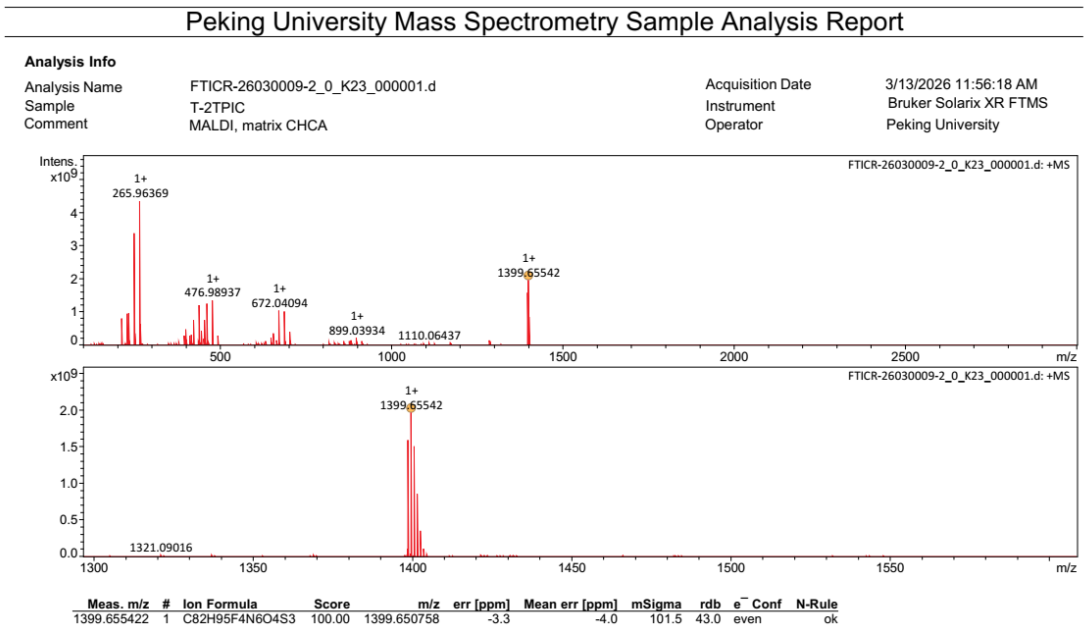


**Fig. S32** HR mass spectrum of T-2TPIC using the MALDI-TOF mode.

**Table S1** Mulliken atomic charge population analysis of T-IC2F

| atom | charge (e) | atom | charge (e) |
|---|---|---|---|
| C1 | –0.135 | O16 | –0.486 |
| C2 | –0.123 | C17 | 0.067 |
| S3 | 0.371 | F18 | –0.267 |
| C4 | –0.346 | F19 | –0.267 |
| C5 | –0.098 | C20 | 0.304 |
| C6 | –0.210 | N21 | –0.499 |
| C7 | 0.042 | C22 | 0.306 |
| C8 | 0.098 | N23 | –0.501 |
| C9 | 0.066 | H24 | 0.175 |
| C10 | 0.061 | H25 | 0.190 |
| C11 | 0.353 | H26 | 0.160 |
| C12 | –0.274 | H27 | 0.195 |
| C13 | 0.339 | H28 | 0.209 |
| C14 | 0.335 | H29 | 0.189 |
| C15 | –0.254 | | |

**Table S2** Mulliken atomic charge population analysis of TT-IC2F

| atom | charge (e) | atom | charge (e) |
|---|---|---|---|
| C1 | –0.217 | C17 | 0.066 |
| C2 | –0.132 | F18 | –0.268 |
| C3 | –0.123 | F19 | –0.267 |
| S4 | 0.356 | C20 | –0.114 |
| C5 | –0.142 | C21 | –0.332 |
| C6 | –0.128 | S22 | 0.285 |
| C7 | 0.041 | C23 | 0.303 |
| C8 | 0.098 | N24 | –0.501 |
| C9 | 0.066 | C25 | 0.306 |
| C10 | 0.062 | N26 | –0.504 |
| C11 | 0.354 | H27 | 0.185 |
| C12 | –0.274 | H28 | 0.193 |
| C13 | 0.338 | H29 | 0.209 |
| C14 | 0.334 | H30 | 0.188 |
| C15 | –0.255 | H31 | 0.169 |
| O16 | –0.487 | H32 | 0.192 |

**Table S3** Mulliken atomic charge population analysis of TP-IC2F

| atom | charge (e) | atom | charge (e) |
|---|---|---|---|
| C1 | –0.267 | C19 | 0.300 |
| C2 | 0.344 | N20 | –0.506 |
| C3 | –0.161 | C21 | 0.313 |
| C4 | 0.347 | N22 | –0.522 |
| C5 | 0.055 | H23 | 0.158 |
| C6 | 0.083 | H24 | 0.208 |
| C7 | 0.071 | H25 | 0.185 |
| C8 | 0.055 | H26 | 0.188 |
| C9 | 0.354 | C27 | –0.226 |
| C10 | –0.277 | H28 | 0.221 |
| C11 | 0.336 | S29 | 0.270 |
| C12 | 0.333 | C30 | –0.094 |
| C13 | –0.258 | H31 | 0.160 |
| O14 | –0.498 | N32 | –0.576 |
| C15 | 0.061 | C33 | –0.367 |
| F16 | –0.270 | H34 | 0.183 |
| F17 | –0.269 | H35 | 0.183 |
| C18 | –0.350 | H36 | 0.235 |

**Table S4** Mulliken atomic charge population analysis of PT-IC2F

| atom | charge (e) | atom | charge (e) |
|---|---|---|---|
| C1 | –0.142 | F19 | –0.270 |
| C2 | –0.132 | N20 | –0.494 |
| S3 | 0.332 | C21 | –0.330 |
| C4 | –0.135 | C22 | 0.300 |
| C5 | 0.304 | N23 | –0.506 |
| C6 | –0.221 | C24 | 0.304 |
| C7 | 0.038 | N25 | –0.512 |
| C8 | 0.096 | H26 | 0.175 |
| C9 | 0.065 | H27 | 0.189 |
| C10 | 0.062 | H28 | 0.207 |
| C11 | 0.351 | H29 | 0.186 |
| C12 | –0.276 | H30 | 0.178 |
| C13 | 0.336 | H31 | 0.185 |
| C14 | 0.332 | H32 | 0.185 |
| C15 | –0.257 | C33 | –0.238 |
| O16 | –0.489 | H34 | 0.155 |
| C17 | 0.059 | C35 | 0.067 |
| F18 | –0.271 | H36 | 0.165 |

**Table S5** Summary of the GIWAXS parameters for the in-plane and out-of-plane directions of the neat films.

| acceptor | in-plane | | | | out-of-plane | | | |
|---|---|---|---|---|---|---|---|---|
| | *q* (Å$^{-1}$) | FWHM | *d* (Å) | CL (Å) | *q* (Å$^{-1}$) | FWHM | *d* (Å) | CL (Å) |
| B-2TPIC | 0.357 | 0.062 | 17.6 | 91.2 | 1.78 | 0.198 | 3.53 | 28.6 |
| T-2TPIC | 0.344 | 0.088 | 18.3 | 64.3 | 1.80 | 0.270 | 3.49 | 20.9 |

**Table S6** Hydrogen evolution performance of advanced organic photocatalytic nanoparticles.

| photocatalyst (mass) | sacrificial agent (solvent volume) | Pt (wt%) | illumination | HER (mmol $h^{-1}$ $g^{-1}$) | ref. |
|---|---|---|---|---|---|
| PTB7-Th:EH-IDTBR (2 mg) | 0.2 M AA (20 mL) | 10 | Xe lamp 350-800 nm | 64 | S9 |
| PM6:Y6 (1 mg) | 0.2 M AA (12 mL) | 10 | AM1.5G 100 mW $cm^{-2}$ | 44 | S10 |
| PM6:$PC_{71}BM$ (2 mg) | 0.2 M AA (12 mL) | 5 | AM1.5G 100 mW $cm^{-2}$ | 75 | S10 |
| PM6:TPP (2 mg) | 0.2 M AA (30 mL) | 20 | AM1.5G 100 mW $cm^{-2}$ | 64 | S11 |
| PM6:Y6CO (0.2 mg) | 0.2 M AA (7.5 mL) | 28 | AM1.5G 100 mW $cm^{-2}$ | 183 | S12 |
| PM6:2FBP-4F (0.18 mg) | 0.2 M AA (7.5 mL) | 24 | AM1.5G 100 mW $cm^{-2}$ | 208 | S13 |
| PM6:B-2TPIC (0.2 mg) | 0.2 M AA (7.5 mL) | 20 | AM1.5G 100 mW $cm^{-2}$ | 152.8 | this work |

**Table S7** The experimental details used for the EQE measurements.

| nanoparticle | wavelength (nm) | radiant power (mW cm$^{-2}$) | radiation area (cm$^2$) | time (s) | $n_h$ ($10^{-6}$ mol) | EQE (%) |
|---|---|---|---|---|---|---|
| PM6:B-2TPIC | 400 | 1.89 | 5.786 | 3600 | 1.67 | 2.5 |
| | 500 | 2.10 | 5.786 | 3600 | 3.13 | 3.4 |
| | 600 | 2.67 | 5.786 | 3600 | 5.73 | 4.1 |
| | 700 | 3.08 | 5.786 | 3600 | 3.98 | 2.1 |
| | 808 | 3.01 | 5.786 | 3600 | 3.62 | 1.7 |
| PM6:T-2TPIC | 400 | 1.89 | 5.786 | 3600 | 1.12 | 1.7 |
| | 500 | 2.10 | 5.786 | 3600 | 1.93 | 2.1 |
| | 600 | 2.67 | 5.786 | 3600 | 5.42 | 3.9 |
| | 700 | 3.08 | 5.786 | 3600 | 4.68 | 2.5 |
| | 808 | 3.01 | 5.786 | 3600 | 4.47 | 2.1 |

## References


S1. X. Zheng, Y. Fu, J. Huang, N. Li, H. Hou, X. Xiao, Y. Lin, X. Lu and X. Zhan, *J. Mater. Chem. C*, 2026, **14**, 3917–3925.

S2. S. Dai, F. Zhao, Q. Zhang, T.-K. Lau, T. Li, K. Liu, Q. Ling, C. Wang, X. Lu, W. You and X. Zhan, *J. Am. Chem. Soc.*, 2017, **139**, 1336-1343.

S3. Gaussian 16, Revision C.01, M. J. Frisch, G. W. Trucks, H. B. Schlegel, G. E. Scuseria, M. A. Robb, J. R. Cheeseman, G. Scalmani, V. Barone, G. A. Petersson, H. Nakatsuji, X. Li, M. Caricato, A. V. Marenich, J. Bloino, B. G. Janesko, R. Gomperts, B. Mennucci, H. P. Hratchian, J. V. Ortiz, A. F. Izmaylov, J. L. Sonnenberg, D. Williams-Young, F. Ding, F. Lipparini, F. Egidi, J. Goings, B. Peng, A. Petrone, T. Henderson, D. Ranasinghe, V. G. Zakrzewski, J. Gao, N. Rega, G. Zheng, W. Liang, M. Hada, M. Ehara, K. Toyota, R. Fukuda, J. Hasegawa, M. Ishida, T. Nakajima, Y. Honda, O. Kitao, H. Nakai, T. Vreven, K. Throssell, J. A. Montgomery, Jr., J. E. Peralta, F. Ogliaro, M. J. Bearpark, J. J. Heyd, E. N. Brothers, K. N. Kudin, V. N. Staroverov, T. A. Keith, R. Kobayashi, J. Normand, K. Raghavachari, A. P. Rendell, J. C. Burant, S. S. Iyengar, J. Tomasi, M. Cossi, J. M. Millam, M. Klene, C. Adamo, R. Cammi, J. W. Ochterski, R. L. Martin, K. Morokuma, O. Farkas, J. B. Foresman, and D. J. Fox, Gaussian, Inc., Wallingford CT, 2016.

S4. T. Lu and F. Chen, *J. Comput. Chem.*, 2012, **33**, 580-592.

S5. T. Lu, *J. Chem. Phys.*, 2024, **161**, 082503.

S6. G. G. Malliaras, J. R. Salem, P. J. Brock and C. Scott, *Phys. Rev. B*, 1998, **58**, 13411-13414.

S7. Y.-T. Yu, J. Wang, J.-H. Zhang, H.-J. Yang, B.-Q. Xu and J.-C. Sun, *J. Phys. Chem. C*, 2007, **111**, 18563-18567.

S8. S. Trasatti, *Pure Appl. Chem.*, 1986, **58**, 955-966.

S9. J. Kosco, M. Bidwell, H. Cha, T. Martin, C. T. Howells, M. Sachs, D. H. Anjum, S. Gonzalez Lopez, L. Zou, A. Wadsworth, W. Zhang, L. Zhang, J. Tellam, R. Sougrat, F. Laquai, D. M. DeLongchamp, J. R. Durrant and I. McCulloch, *Nat.*

*Mater.*, 2020, **19**, 559-565.

S10. J. Kosco, S. Gonzalez-Carrero, C. T. Howells, T. Fei, Y. Dong, R. Sougrat, G. T. Harrison, Y. Firdaus, R. Sheelamanthula, B. Purushothaman, F. Moruzzi, W. Xu, L. Zhao, A. Basu, S. De Wolf, T. D. Anthopoulos, J. R. Durrant and I. McCulloch, *Nat. Energy*, 2022, **7**, 340-351.

S11. Z. Zhang, W. Si, B. Wu, W. Wang, Y. Li, W. Ma and Y. Lin, *Angew. Chem. Int. Ed.*, 2022, **61**, e202114234

S12. Y. Liang, T. Li, Y. Lee, Z. Zhang, Y. Li, W. Si, Z. Liu, C. Zhang, Y. Qiao, S. Bai and Y. Lin, *Angew. Chem. Int. Ed.*, 2023, **62**, e202217989.

S13. Z. Zhang, C. Xu, Q. Sun, Y. Zhu, W. Yan, G. Cai, Y. Li, W. Si, X. Lu, W. Xu, Y. Yang and Y. Lin, *Angew. Chem. Int. Ed.*, 2024, **63**, e202402343.